Acta Geophysica
https://doi.org/10.1007/s11600-025-01665-8

RESEARCH ARTICLE - ATMOSPHERIC & SPACE SCIENCES

Analysis of the temporal pattern of storms in three different climates of Iran

Saina Vakili Azar[1] · **Yagob Dinpashoh**[1] · **Saeed Jahanbakhsh Asl**[2]

Received: 5 January 2025 / Accepted: 2 July 2025

Abstract

Understanding the temporal distribution of rainfall is crucial for effective water management. In this study, the patterns of 1983 historical storms, as recorded at 16 rain gauge stations across three climatic regions in Iran, were analyzed. Huff curves were plotted for the stations in three distinct classes. The binary shape code method was used to detect storm patterns. Six newly defined ratios were calculated for each station based on the area under the median Huff curve in the four quartiles. Results showed that for most stations, the storms were identified as second, followed by the third quartile. The differences between the means of the dimensionless rainfalls in each quartile were tested between three possible pairs of climates in Iran. For storms with less than a six-hour duration, there was no significant difference between any pair of climates for all four possible quartiles. For storms with 6–12 h durations, similar results were found for the first and second quartiles. In the third quartile, the averages between the semi-humid and semi-arid climates of Iran were dissimilar. For fourth quartile storms, there was no similarity between the humid and semi-humid climates on one side and the humid and semi-arid climates on the other side. For more than 12-h class storms, although there was a statistically significant difference in the second quartile between the pairs of climates, no significant difference was found for the 3rd quartile. About half of the tests in the 1st and 4th quartiles passed the test for averages of dimensionless rainfall depths between the pairs of climates; however, the remaining cases failed. In most of the events, the binary code was 0111 in humid and semi-humid climates. The code was 1111 in a semi-arid climate using the first mode of the binary approach. In the second mode, and for all three climates, the highest frequency belonged to code 1111, followed by codes 0000, 0111, 0011, and 0001, respectively. According to the dendrogram, the first group of storms, i.e., "< 6 h", had three distinct clusters. The second group of storms, i.e., "6–12 h," also had three distinct clusters, however, the third group had four distinct clusters.

Keywords Binary method · Climate · Cluster · Huff curve · Storm analysis

Introduction

A deep understanding of the temporal pattern of storms is very important in drainage design, hydrological modeling, pollution transport, erosion control, rainwater harvesting, flood diversion, and flood hazard prediction (Azli and Rao 2010; Terranova and Iaquinta 2011; Abraham et al. 2015; Dolsak et al. 2016). It is also important in simulating runoff hydrographs in the basins (especially urban basins). If a substantial part of the rainfall event occurs in the first half of its duration, the peak river discharge is lower than when most of the precipitation occurs in the second half of the period (Dolsak et al. 2016). By converting the duration and depth of storms into their non-dimensional form, it is possible to compare the types of storms in different climates. Studying the temporal structure of precipitation events is significant in

Edited by Dr. Ahmad Sharafati (ASSOCIATE EDITOR) / Prof. Theodore Karacostas (CO-EDITOR-IN-CHIEF).

✉ Yagob Dinpashoh
dinpashoh@yahoo.com

Saina Vakili Azar
sainavazar@yahoo.com

Saeed Jahanbakhsh Asl
jahanbakhshsaeed@yahoo.com

[1] Department of Water Engineering, University of Tabriz, Tabriz, Iran

[2] Department of Geography, University of Tabriz, Tabriz, Iran

Published online: 29 July 2025

soil erosion and flash flood analyses. Understanding the temporal distribution patterns of precipitation is also important in hydrological modeling (Terranova and Iaquinta 2011).

Many researchers have studied the time distribution patterns of precipitation. One research method uses Huff curves (Huff 1967). According to 300 storms from 50 selected stations in the USA, Hirschfield (1962) studied the pattern of storms in four different precipitation classes. The results indicated that the time distribution of American precipitation is not the same in different stations. In the eastern part of Illinois State in the USA, with a selection of 261 precipitation events from 49 rain gauge stations, a study was conducted by Huff (1967) on the temporal distribution pattern of storms for a time period of 11 years. The results revealed that the highest percentage of storms had a duration of less than 12 h (Huff 1967).

The temporal distribution pattern of storms was investigated using 45,533 storms recorded during 1989–2008 in the Calabria region in southern Italy, and the standardized precipitation profile (SRP) method was used, which was based on accurate and local precipitation data. The storms were divided into different precipitation classes based on their duration, and then their Huff curves were plotted. The areas under the SRP curve in each of the four quartiles of duration were denoted by A_1 to A_4, respectively, which were then calculated. These areas were compared with the corresponding areas of the uniform standardized precipitation profile (USRP). A new criterion called the binary shape code (BSC) method was presented by Terranova and Iaquinta (2011). Over a statistical time period of twenty years, the pattern of precipitation distribution was obtained using rain gauge stations of Makkah Al-Mukkramah (Ewea et al. 2016). Their results revealed that most precipitation occurs in the first and second quartiles in the region. In another study, the temporal distribution patterns of precipitation were investigated using methods including Huff curves and binary coding methods for three different climates of Slovenia (Dolsak et al. 2016). The results showed that for the storms with a duration of less than 12 h, the code was 1111. However, it was 0000 for the storms with a duration of more than 12 h (Dolsak et al. 2016).

Many storms were investigated in a region located in the northwest region of Croatia to estimate flood hydrograph ordinates (Krvavica and Rubinic 2020). In another study, changes in precipitation in Wenchuan County, China, were analyzed based on 817 storms using Huff curves (Xlong et al. 2021). The effect of these changes on the peak discharge of floods was investigated using the HEC-HMS coupled model. The results disclosed that the peak discharges gradually increase from the 1st to the 4th quartiles in the region (Xlong et al. 2021). The standard Huff curve was modified by Dunkerley (2022). In that work, only precipitation events whose durations were greater than a certain threshold were considered for analysis. According to this method, it was found that in some cases, by applying the new criterion, an event that previously belonged to the first quartile shifted to the fourth quartile (Dunkerley 2022). In another study, Nguyen and Chen (2022) modified the conventional Huff curve. With this method, more events were used in the analysis than with traditional methods. The results demonstrated that the modified method distinguishes precipitation events, and the characteristics of artificial precipitation are very similar to reciprocal historical events in the region (Nguyen and Chen 2022).

Other similar studies have been conducted in Iran for storm analysis using different methods. Among them, we refer to the works of Hatami Yazd et al. (2005) in plotting Huff curves in Khorasan province, Khaksafidi et al. (2011) in the Sistan and Baluchestan province, Baniasadi (2011) in the Kerman province, Karimi et al. (2013) in Babolsar, Moradnezhadi et al. (2016) at Nowshahr station, Dinpashoh and Vakili Azar, (2019) and Vakili azar and Dinpazhoh (2019) for stations located east of Urmia Lake, Alavi et al. (2019) in Khuzestan province, and Dinpashoh and Alavi (2024) in Great Karoun River basin in Iran. Mojaradi Gilan et al. (2010) studied the impact of the time distribution pattern of precipitation on runoff and sediment production using a rainfall simulator. They first analyzed the time distribution patterns of Alvand watershed storms and then compared the results with the American Soil Conservation Service (SCS) patterns. Based on the results, no similarity was seen between SCS-type and regional patterns. Likewise, the results disclosed that the correlation between sediment variables, runoff, and the runoff coefficient depends on the changes in the precipitation patterns in the simulation formula (Mojaradi Gilan et al. 2010).

The time distribution pattern of precipitation in Iran has been investigated by plotting Huff curves. However, the use of the binary method in comparing precipitation patterns in different climates of Iran has not been investigated and discussed. Since Iran is a large country with different climates, considering the climatic changes and the problems with water shortage, especially in semi-arid areas, this study is important for optimal management of water resources and prevention of possible risks such as flash floods. In the present study, the time distribution patterns of precipitation are presented by Huff curves and analyzed by using the binary method in two distinct stages. New ratios will be defined in this study based on the area under the Huff curves for different quartile storms in each of the stations. This method allowed storms to be classified into different clusters using the hierarchical Ward method. Newly defined ratios in the present study are used as input in the clustering method for partitioning the storm patterns. This approach has not been used before by other researchers. Therefore, the

objectives of this study are: (1) plotting Huff curves for identification of storm types in terms of quartiles, (2) application of the binary method to distinguish the type of rainfall events, (3) defining and calculating the new ratios based on areas under the median Huff curve in each of the quartiles, and (4) clustering the stations based on the aforementioned ratios using the Ward method to investigate the similarity of rainfall patterns.

Materials and methods

Study area

Iran is a vast country having diverse climates. The patterns of rainfall in these climates differ. To our knowledge, the rainfall patterns of different climates of Iran have not been comprehensively studied. This study analyzes the storm patterns in three distinct climatic zones using an innovative approach, namely the binary method. Three important Iranian climate zones are identified: (1) humid, (2) semi-humid, and (3) semi-arid. The arid climate of Iran, which includes a vast portion of Iran, is not considered here due to insufficient available rainfall records. The study area selected in the present research incorporated three distinct climates. The first one is the humid climate, including two provinces, namely Gilan and Mazandaran located in northern Iran near the Caspian Sea (the western and central shores). This region has more annual rainfall than all other parts of Iran (Dinpashoh et al. 2004). More specifically, the mean annual precipitation in the Gilan province is 1100 mm (Khosravi et al. 2013), > 1000 mm west of Mazandaran province, and > 300 mm in the east of the province (Farsadnia et al. 2012). The second selected climate is semi-humid and includes two distinct provinces located far from each other. The name of the first province is Golestan, situated in northern Iran (on the eastern shores of the Caspian Sea). The mean annual precipitation of this province is 530 mm (Bazrafshan Daryasari et al. 2016). The second one is the Kohgiluyeh-va-Boyer Ahmad (KvB) province, located in the west of Iran. This province has a mean annual rainfall of about 550.7 mm, according to Salehi et al. (2017). The third region incorporated in the present study is the semi-arid climate. Among different parts of Iran having semi-arid climates, the East Azerbaijan (E-Az) province located in the northwest of Iran is selected here. The mean annual precipitation of this province is reported to be between 250 and 300 mm (Mirabadi et al. 2017). From these climate zones, sixteen rain gauge stations were selected, of which six sites belonged to the humid climate. Similarly, six sites were chosen from the semi-humid climate, and four sites were selected from the semi-arid climate. All the selected sites had sufficient data for analysis. Figure 1 shows the geographical location of the selected provinces and stations from different climates of Iran.

Data used

Rainfall records are measured routinely by automatic rain gauge stations in Iran. Two distinct organizations are responsible for this task: (1) the IRAN Water Resources Management Company (IRAN WRMC) and (2) the Islamic Republic of Iran Meteorological Organization (IRIMO). As the IRIMO's rainfall data had a relatively low resolution (10 min) compared to IRAN WRMC's (1 min), so the latter was prioritized over the former. Complete series of events in 1-min resolution with no missing value in the period 2001–2019 provided by IRAN WRMC in an Excel file. All the data were checked for accuracy and underwent quality control. Several technical issues were encountered during the measurement process. For example, due to the malfunction of rain gauges, several rainfall events in consecutive months are not provided. These cases were not considered as "Missing data". In addition, in some instances, where the cumulative rainfall depth was far greater than the normally measured rainfall depth is not considered for analysis.

A total of 1983 events from 16 different stations were used in the analysis. For each storm, cumulative precipitation curves were converted into precipitation depth per minute by the IRAN WRMC. The rainfall data have a depth resolution of millimeters (mm). Table 1 outlines the geographical characteristics of the selected stations. Figure 2 shows a histogram showing the number of storms recorded in each of the three storm groups across three distinct climates of Iran. Based on Fig. 2, the highest number of storms used in this study corresponds to the humid climate, having a total number of storms equal to 926. The second rank belonged to the semi-arid climate with 554 storms. The third rank related to the semi-humid climate, having 503 storms, was used in the present study. According to Fig. 2, in the group of "less than 6" hours rainfall duration class, the highest number of storms belonged to the semi-arid climate, having 435 storms. In this class humid climate had 317 storms, while the lowest number of storms in this group belonged to the semi-humid climate, having 203 storms. As can be seen from Fig. 2, in the group of "6–12 h" storms, the highest number of storms belonged to the humid climate, having 319 storms. In this class, the semi-humid climate had 147 storms, while the lowest number of storms in this group belonged to the semi-arid climate, having 88 storms. As can be deduced from Fig. 2, in the group of "> 12 h" storms, the highest number of storms belonged to the humid climate,

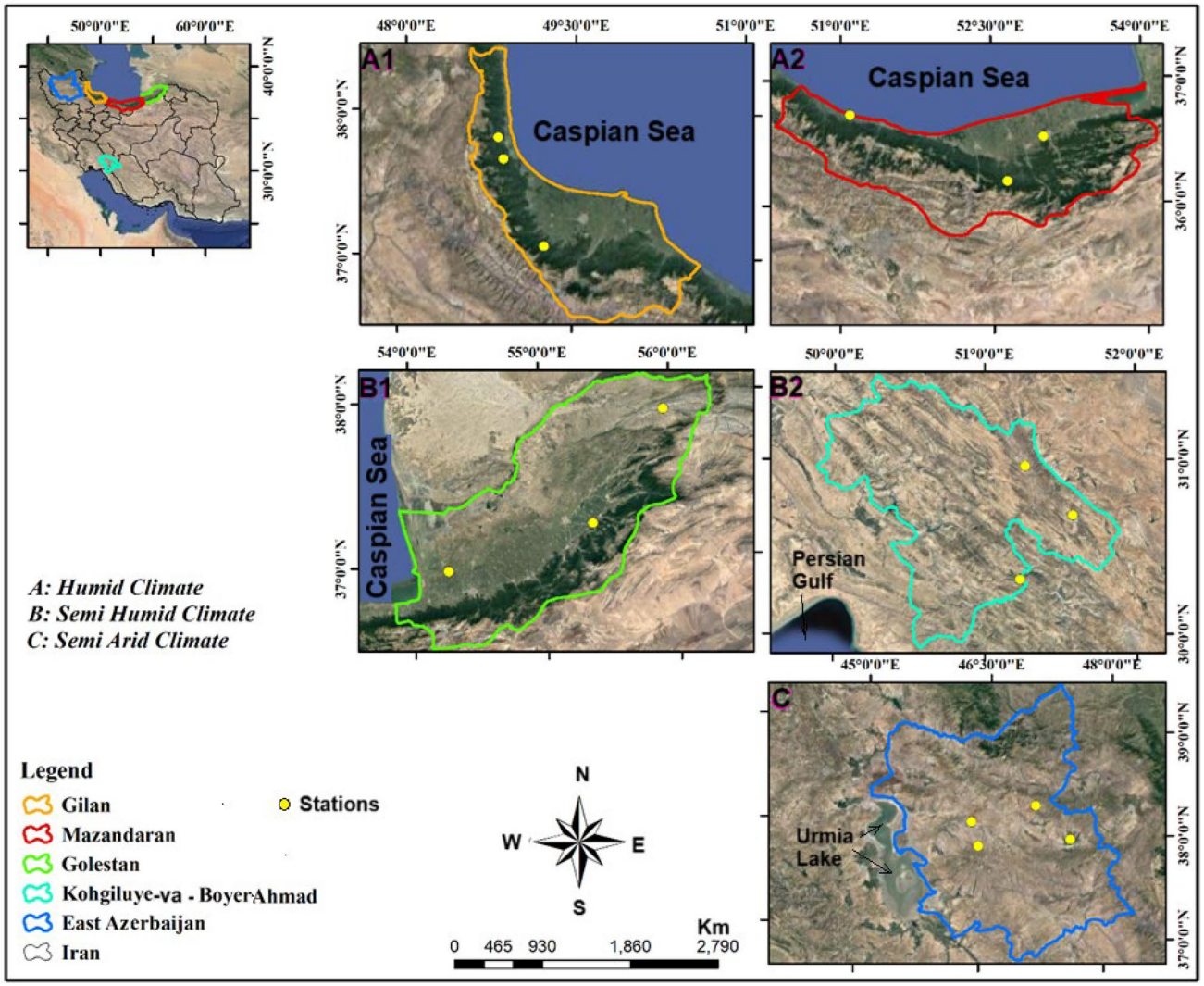

Fig. 1 The geographical locations of the selected stations in the three distinct climates of Iran: **A1**—Gilan province (humid climate), **A2**—Mazandaran province (humid climate), **B1**—Golestan province (semi-humid climate), **B2**—Kohgiluyeh-va-Boyer Ahmad (KvB) province (semi-humid climate), and **C** East Azerbaijan (E-Az) province (semi-arid climate)

having 290 storms. In this class, the semi-humid climate had 153 storms, while the lowest number of storms in this group belonged to the semi-arid climate, having 31 storms. It can be seen that low-duration storms (i.e., < 6 h) had a greater number of events compared to the moderate (i.e., "6–12 h") and high-duration (> 12 h) events.

Identification of independent rainfall events

Before analyzing storms at a given station, there is a need to define a criterion to identify independent events. In a given storm, continuous bursts of rain are separated by periods of no rain (or dry spells). In a given storm, such a dry spell of the order of minutes would be attributed to the same event. However, bursts of rain separated by dry spells of the order of hours (for example, more than six hours) would not relate to the same storm. A minimum dry period between two subsequent storms should be defined to identify independent events. Most researchers used a minimum time distance (for example, 6 h) between the two subsequent storms for this aim. For example, Huff (1967) and Huff (1990) in the eastern state of Illinois, Terranova and Iaquinta (2011) in Calabria (southern Italy), and Dolsak et al. (2016) in Slovenia used a constant time interval of 6 h to distinguish different storms. Thus, if the rain end time of a given event exceeds 6 h, the subsequent event is considered independent from the previous one. Wu et al. (2006) considered a 2-h cessation of rainfall in Hong Kong. Bonta (2001) supposed that this time can vary depending on the season. He investigated the time

Table 1 Geographical characteristics of the selected stations, the average annual precipitation, data time period, and the number of events in the three distinct climates of Iran

Climate	Province	Station	Latitude	Longitude	Altitude (m)	Annual rainfall (mm)	time period	No. of events
	Mazandaran	Sari	36°32′	53°01′	17	792.1	2009–2017	164
		Abbas Abad	36°44′	51°06′	− 18	1487.7	2009–2017	151
		Firuzjah	36°11′	52°39′	787	966.4	2009–2017	249
Humid								
	Gilan	Kharfehgil	37°41′	48°53′	145	1239.7	2008–2014	80
		Qaleh Rudkhan	37°05′	49°15′	186	1732	2008–2016	170
		Hashtpar	37°50′	48°50′	99	1200	2008–2014	112
	Golestan	Aqqala	37°58′	54°16′	12	415.8	2009–2016	123
		Maraveh Tappeh	37°54′	55°57′	218	361	2010–2017	66
		Minudasht	37°14′	55°22′	167	770	2010–2017	135
Semi-humid								
	KvB*	Pataveh	30°58′	51°16′	1550	485	2004–2017	72
		Tang berim	30°19	51°14′	750	704	2005–2016	70
		Yasuj	30°41′	51°35′	1850	843	2004–2016	37
	E-Az**	Tabriz	38°04′	46°20′	1413	238.6	2001–2019	97
Semi-arid		Heris	38°15′	47°07′	1965	346.7	2001–2018	186
		Sarab	37°56′	47°33′	1686	181.9	2003–2018	103
		Liqvan	37°50′	46°26′	2274	352.7	2004–2019	168
								Sum = 1983

*KvB is the Kohgiluyeh-va-Boyer Ahmad province, and **E-Az is the East Azerbaijan province

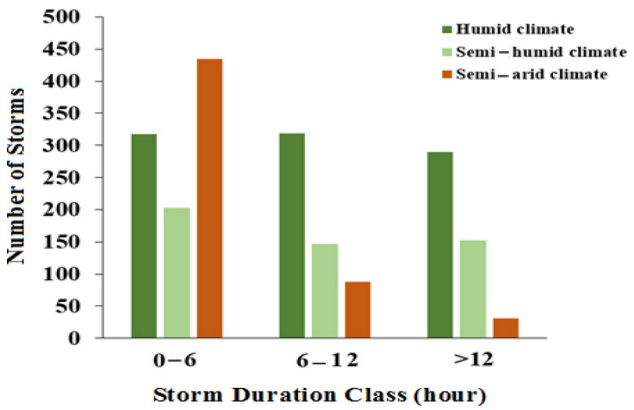

Fig. 2 Histogram of the number of storms recorded in each of the three precipitation classes and three different climates of Iran

interval between the two adjacent storms and reported that this time varies from 16.5 to 26.9 h over the plain area of Colorado. Patino et al. (2023) used the autocorrelation function to define the independent adjacent storms. In the present study, a constant time of six hours was used as a minimum time distance between two subsequent events to identify different storms. Figure 3a shows the rainfall bursts and inter-storm periods in distinguishing the independent storms.

It is important to select a logical number of events for analysis in each of the climates of Iran. It is also very important to know that the number of events in arid (or semi-arid) climates is low compared to the other climates. Therefore, by selecting a high value for the minimum depth of rain, the number of storms would be decreased. This led to plotting the Huff curve with such a low number of events, which in turn plotted Huff curves are not reliable and useful for further practical purposes. This is so important for the semi-arid climate of Iran, in which the number of events is less than in the other climates. After selecting such a threshold for the semi-arid climate, a similar decision was used for the semi-humid and later for the humid climate in Iran. By this practice, a sufficient number of rainfall events were provided for plotting Huff curves in each climate in Iran.

In most studies, the cumulative depth of rainfall threshold of 12.7 mm suggested by Huff (1967) is applied to obtain comparable results with similar works. However, as different climates of Iran have different mean rainfall depths in the present study, different criteria for identifying storms are used, which are:

a. In a humid climate, the minimum depth of precipitation is considered to be 5 mm, and its duration is at least 60 min.

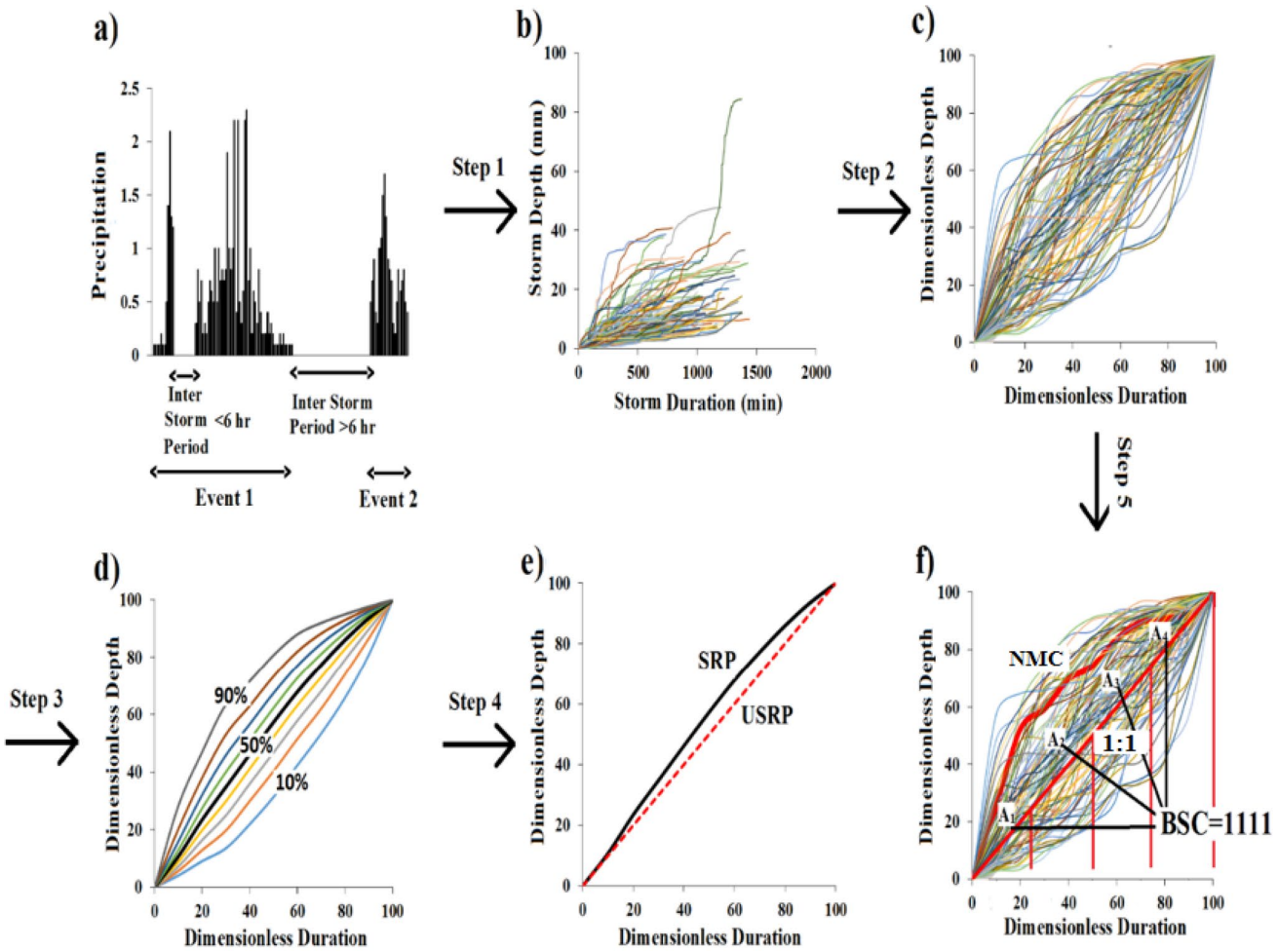

Fig. 3 Huff curves preparation stages (**a**–**d**) and using the BSC method (e and f) for analyzing the storms in a sample station, namely Firuzjah, having a humid climate located in Mazandaran province

b. In a semi-humid climate, the minimum depth of precipitation is considered to be 4 mm, and its duration is at least 60 min.
c. In a semi-arid climate, the minimum depth of precipitation is considered to be 3 mm, and its duration is at least 20 min.

Different steps for plotting the Huff curves are explained in the following subsection.

Huff curves

Huff curves are probabilistic time distributions of rainfall expressed as dimensionless cumulative percentages of storm depth and duration. To develop Huff curves, short-time increments on the order of minutes should be used. In this study, Huff curves were developed for each site and each of the three rainfall classes, including: (1) less than 6, (2) 6–12, and (3) more than 12 h.

Figure 3 schematically shows different stages of Huff curve preparation (a, b, c, and d) in a sample station, Firuzjah, located in the humid climate of Mazandaran province. Furthermore, the last two stages (e and f) belonged to the binary method explanation on the mentioned site. Figure 3e shows two distinct curves, which are the median Huff curve (also called SRP) and the 1:1 line (USRP). The position of these two curves compared to each other in the four quartiles characterizes the binary codes. Detailed explanation of Fig. 3e is represented in Sect. 2.5.1 (first mode approach). Figure 3f shows several nondimensional mass curves (NMC) of storms as well as the representative one, which is compared to a 1:1 line, used to detect the binary shape codes of the storm in the second mode approach. This approach is described later in detail in Sect. 2.5.2.

After the classification of the storms by the abovementioned criteria shown in Fig. 3a, all events in the form of mass curves are considered for a single site (Fig. 3b). Each mass curve in Fig. 3b is nondimensionalized by dividing all

breakpoint cumulative depths by the total rainfall depth. The resulting plots are shown in Fig. 3c for a representative station. By adding probability to the dimensionless mass curve, the order is made of the apparent disorder in Fig. 3d. Huff curves were plotted by fitting different statistical distributions to data corresponding to nine probabilities, which are the 10, 20,…, and 90 percentiles (Fig. 3d). This was accomplished for each of the three aforementioned classes and the selected stations. After plotting the Huff curves, the 50% Huff curve, also called the median Huff curve, was identified. From this median curve, the percentage of precipitation received in each of the four quartiles was calculated. Then, the averages of precipitation percentages received in the quartiles were calculated in three distinct climates and the rainfall classes. Then, these values were compared in the cases of different climates and/or classes. This issue is explained in detail in the following subsection.

Comparing the means

To compare the means of two distinct groups (climates and/or classes), the T_c statistic is calculated from Eq. (1). Suppose there are two distinct hydrologic series. The first series x_t, $t=1, 2, \ldots, N_1$ has mean μ_1 and standard deviation σ and the second series x_t, $t=1, 2, \ldots, N_2$ has mean μ_2 and standard deviation σ. The simple t-test can be used to test the hypothesis $\mu_1=\mu_2$ when both of the series have the same standard deviation. In this regard, T_c is calculated from the following equation (Salas 1993):

$$T_c = \frac{|\bar{x}_2 - \bar{x}_1|}{S\sqrt{\frac{1}{N_1}+\frac{1}{N_2}}}, \tag{1}$$

where N_1 and N_2 are the number of observations of the first and second groups, and $\bar{x}_1$ and $\bar{x}_2$ are the means of the first and second groups, respectively. The statistic S in Eq. (1) is calculated from the following equation:

$$S = \sqrt{\frac{(N_1-1)S_1^2 + (N_2-1)S_2^2}{N-2}}, \tag{2}$$

where ${S_1}^2$ and ${S_2}^2$ are the variances of the first and second groups, respectively, and $N=N_1+N_2$. If $T_c > T_{1-\alpha/2}$, the null hypothesis (H_0), i.e., $\mu_1=\mu_2$ would be rejected, and the opposite hypothesis (H_1), i.e., $\mu_1 \neq \mu_2$, would be accepted. Otherwise, if $T_c \leq T_{1-\alpha/2}$, the null hypothesis would be accepted. Here, $T_{1-\alpha/2}$, extracted from the Student's t Table with a degree of freedom equal to N_1+N_2-2 and a significance level of $\alpha/2$.

Binary method

The binary method was used here for pattern recognition of storms in two distinct modes. These two modes are explained in the following subsections.

First mode approach

After plotting the Huff curves for the stations, the median Huff curve (SRP) is considered in the first approach. The mathematical form of the SRP is obtained. The model suitability was checked using two criteria, R^2 and standard error. In this mode, in addition to SRP, the 1:1 line (also called USRP) was plotted in the same diagram (Fig. 3e). Storms were identified using the binary method (as discussed in Terranova and Iaquinta 2011) according to the SRP and USRP curves. For example, if SRP is positioned above the 1:1 line in the first quartile, the digit 1 is attributed to that quartile. Otherwise, the digit 0 is used. A similar process is used for the second, third, and fourth quartiles. With this method, a four-digit binary code (0 and/or 1) is attributed to each site. In general, sixteen binary codes describe the pattern of storms. For instance, consider a hypothetical storm in which the areas under the SRP curve in the first and third quartiles were greater than the corresponding areas under the USRP line, and the areas under the SRP curve in the second and fourth quartiles were less than the corresponding areas under the USRP line, the code 1010 can be attributed to this station. In the current study, all the stations were analyzed using the first mode of the BSC method.

The area under the median Huff curve in each of the four quartiles was calculated using Eq. (3). Four distinct intervals considered in the integration of $f(x)$, which are: (1) for the first quartile from $\tau_l=0$ to $\tau_u=0.25$, (2) for the second quartile from $\tau_l=0.25$ to $\tau_u=0.5$, (3) for the third quartile from $\tau_l=0.5$ to $\tau_u=0.75$, and (4) for the fourth quartile from $\tau_l=0.75$ to $\tau_u=1$. The integral of the jth quartile reads:

$$I_j = \int_{\tau_L}^{\tau_U} f(x)\mathrm{d}x, \quad j = 1, 2, \ldots, 4, \tag{3}$$

where j is the number of quartiles, and τ_L and τ_u are the lower and the upper limits of the integral, respectively. Similar to SRP, the area under the USRP in different quartiles was calculated. By comparing the I_j values obtained for a given site for the SRP and USRP, the digits (0 or 1) were attributed to each of the four quartiles. In this way, the binary code corresponding to the SRP and 1:1 line (USRP) is assigned to each of the selected stations (Fig. 3e). If Ij obtained for SRP is greater than I_j of USRP, then digit 1

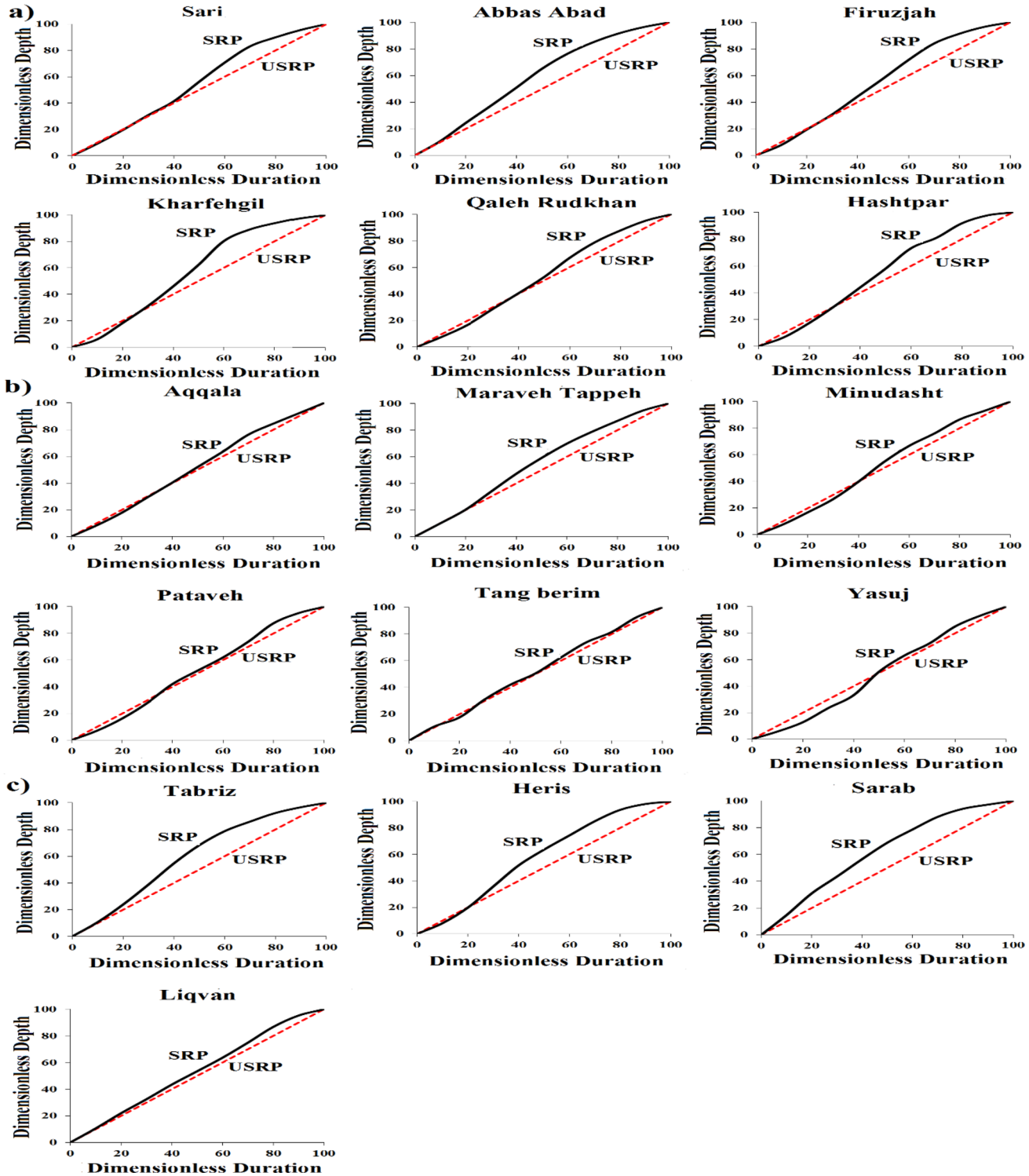

Fig. 4 The 50% Huff curve (SRP) and the 1:1 line (USRP) in a sample class (less than 6 h) at selected stations

is considered for the jth quartile, otherwise, 0 is attributed to that quartile. Finally, a four-digit code containing 0 and/or 1 is assigned for the site. For example, Fig. 4 shows the pairs of curves (SRP and USRP) in the case of the first class of storms (i.e., less than 6 h duration) for all 16 selected stations.

Second mode approach

In the second mode of the binary method, each of the 1983 storms is considered separately. Consider a given storm, a pair of curves was plotted in a single diagram. The first is the nondimensional mass curve (NMC) for a given event (rainfall), and the second is a 1:1 line. The position of the area bounded between the two mentioned curves was inspected visually in the quartiles. If most of the area between NMC and the 1:1 line lies below the bisector line, then the digit 0 is used; otherwise, the digit 1 is attributed to the quartile. Therefore, a four-digit code (0 and/or 1) is assigned for the storm. All the storms were coded for each of the 16 selected sites. 1983 binary codes, equal to the total number of storms, were classified this way. An example can be seen in Fig. 3f.

At a given site, the frequency of BSCs was counted for each of the 16 possible codes. Results were tabulated for each of the stations. Then, for a given station, the relative frequencies (in percentages) of all the sixteen BSC types were illustrated as pie plots. For example, Fig. 5 depicts the pie plots in a sample station, Firuzjah, for the three classes**.** Based on Fig. 5, the binary code 1111 has the highest percentage of storms in all three classes. As can be seen from Fig. 5, as the duration class of rain increases from less than 6 h to more than 12 h, the percentage of frequency of the 0000 code increases as well, which is in accord with the findings of Dolsak et al. (2016). These obtained codes can be used as inputs to hydrological models to simulate precipitation-runoff models (Dolsak et al. 2016).

Defining new ratios

Six new ratios were introduced here to check and identify the similarity of storm patterns in different stations. These ratios are introduced here as a novelty of this study. These newly defined ratios were used as input in the clustering of the stations. After calculating I_1, I_2, I_3, and I_4 (Eq. 3), the values of six new ratios (I_2/I_1, I_3/I_1, I_3/I_2, I_4/I_1, I_4/I_2, I_4/I_3) were calculated. These six ratios were denoted here by R1-R6. They were used to calculate the Euclidean distances between the stations. Based on these distances, stations were classified by a clustering procedure using the Ward method. This procedure is explained in the following subsection.

Clustering analysis

Cluster analysis finds groups of storms that are similar to each other in a given cluster but dissimilar from other clusters. After calculating the newly defined ratios, they were used as input for the cluster analysis. A common method to identify groups in a dataset is Ward's hierarchical method (Ward 1963). This approach considers the Euclidean distances to events with similar rainfall. Using the previously defined ratios (R_1, …, R_6), all stations are classified into distinct clusters. This analysis is performed using the Euclidean distance (D_{ij}) between the stations. For measuring the distance between the ith and jth stations, the following equation is obtained:

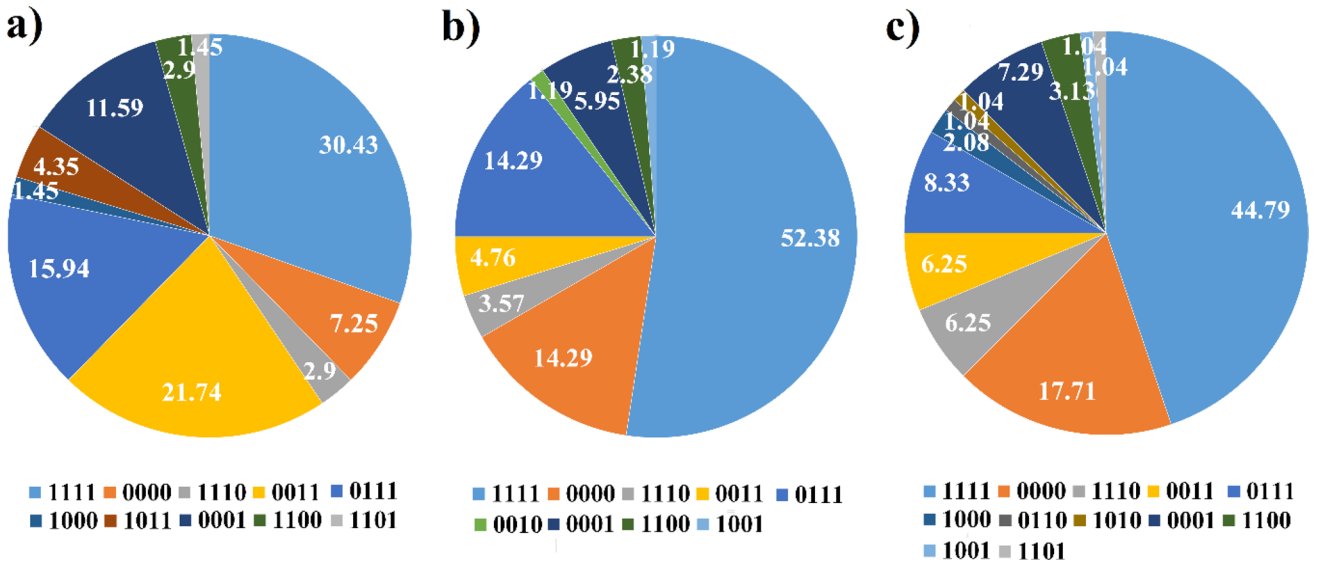

Fig. 5 The pie plots of the relative frequencies (in percentages) in different rainfall classes, **a** less than 6 h, **b** 6–12 h, and **c** more than 12 h in the station Firuzjah located in Mazandaran province

$$D_{ij} = \sqrt{\left(R_{1i} - R_{1j}\right)^2 + \left(R_{2i} - R_{2j}\right)^2 + \ldots \left(R_{6i} - R_{6j}\right)^2}; \quad \text{for} \quad i,j = 1, 2, \ldots, 6. \tag{4}$$

The two stations having the minimum distance were joined together. Once again, the Euclidean distance of the stations was calculated along with the newly established cluster, and the two stations (or clusters) that had the minimum distance were joined together. The resulting dendrogram of the stations in each of the three classes was plotted.

Results and discussion

Huff curves

As mentioned in the methods section, after selecting individual storms according to climatic conditions, all the 1983 recorded storms at the 16 stations (Table 1) were divided into three distinct precipitation classes according to the storm duration (Fig. 2). Then, the set of dimensionless curves was plotted with the cumulative precipitation depth as the vertical axis and the cumulative time as the horizontal axis. Results showed that as the number of storms increased, the resultant curves became smoother. Table 2 represents the precipitation percentages received at each station in different quartiles. In preparing the mentioned table, the 50% Huff curve was used.

As can be seen from Table 2, three different storm classes are considered. According to Table 2, for storms shorter than 6 h in the humid climate, all but one station (namely, Qaleh Rudkhan) showed the second quartile rainfall patterns. Also, for a semi-humid climate, all but one station (namely, Tang Berim) represented the second quartile patterns. For the semi-arid climate, storms of the two stations (namely Tabriz and Heris) exhibited the second quartile patterns.

For storms of 6–12 h in the humid climate, all but two stations (namely Sari and Kharfehgil) had the second quartile rainfall patterns. For the semi-humid climate, all the stations in Golestan province had a second quartile pattern type. However, the Pataveh station, located in the KvB province, showed a first quartile pattern. The Tang Berim station represented the third quartile pattern, and the Yasuj station exhibited the fourth quartile pattern. In the semi-arid climate, except for Tabriz station, which showed the third quartile pattern, other stations had second quartile rainfall patterns.

For storms having a duration of > 12 h in a humid climate, the type of storm for all but one station (Firuzjah) was identified as the second quartile. This result is in agreement with the findings of Moradnezhadi et al. (2016). Their results are similar to the present study. In the same class and a semi-humid climate, two stations (namely Pataveh and Tang Berim) showed storm patterns of the third quartiles, but the rest of the stations were identified as second quartiles. In the same class and a semi-arid climate, two stations (namely Tabriz and Sarab) exhibited first quartile patterns. The Heris station showed the second quartile pattern, and the Liqvan station represented the third quartile pattern type.

Ewea et al. (2016) reported that storms at a station called Makkah Al-Mukkramah, which has an arid climate, exhibited first and second quartile type patterns. In this study, Huff curves are not plotted due to a lack of recorded storms in the arid climate. Todisco (2016) found that 66 out of 227 storms at a station called Masse (located in the center of Italy with a humid climate) receive a substantial part of the rainfall in the first half of their duration. This is in agreement with the findings of the present study. Wang et al. (2016) examined precipitation patterns related to 84 storms between 2006 and 2013 in Beijing, China. They reported that about 40% of the precipitation in Beijing falls in the first third of the precipitation time period. These observations agree with the present study's findings for humid climates. Hatami Yazd et al. (2005) reported that in Khorasan province, located in northeast Iran, which has a semi-arid climate, more than 50% of precipitation occurs in the first half of the storm duration. This report is in line with the findings in the present study for most of the stations located in the semi-arid climate (E-Az province).

In the present study, averages of rainfall percentages received in different quartiles were calculated for three aforementioned duration classes and three different climates of Iran. The averages were compared to different climates at the 5% level. This was accomplished for different rainfall classes. Table 3 shows the results of the pairwise comparison of averages of rainfall percentages received in different quartiles. As seen from the table, for the rainfall duration class of less than 6 h, there was no significant difference in the average of received rainfall percentages between any two climates in Iran. This is true for all four quartiles between any two climates. In other words, the precipitation patterns in all four quartiles are similar to each other. In the case of the 6–12 h storms, the dimensionless rainfalls were not significantly different between any two climates of Iran in the first and second quartiles. However, it is not valid for the other quartiles. In the third quartile, such similarity was not found between the semi-humid and semi-arid climates of Iran. For the fourth quartile, there was no evidence of similarity between the humid and semi-humid climates on one side, and the humid and semi-arid climates on the other side.

Table 2 The percentage of rainfall depth received in different time quartiles, in each of the precipitation classes for the selected stations in different climates of Iran using the Median Huff curve

Climate	Province	Station	Quartile			
			First	Second	Third	Fourth
Less than 6 h						
Humid	Mazandaran	Sari	25.31	**31.01**	30.24	13.46
		Abbas Abad Firuzjah	31.01	**34.21**	23.12	11.66
			25.12	**32.61**	30.06	12.21
	Gilan	Kharfehgil	24.73	**37.55**	29.01	8.71
		Qaleh Rudkhan	22.75	29.89	**30.74**	16.63
		Hashtpar	23.72	**34.28**	28.46	13.56
Semi-humid	Golestan	Aqqala	23.48	**28.58**	28.34	19.61
		Maraveh Tappeh	26.99	**32.15**	23.83	17.03
		Minudasht	21.76	**32.78**	26.8	18.67
	KvB	Pataveh	22.1	**30.02**	28.61	19.28
		Tang Berim	24.29	26.26	**27.13**	22.33
		Yasuj	18.09	**32.8**	27.93	21.18
Semi-arid	E-Az	Tabriz	31.3	**36.91**	20.95	10.86
		Heris	27.81	**35.84**	25.75	10.61
		Sarab	**37.2**	31.62	22.3	8.89
		Liqvan	27.19	26.28	**27.38**	19.15
6–12 h						
Humid	Mazandaran	Sari	**29.93**	28.9	27.12	14.05
		Abbas Abad	28.41	**32.13**	24.29	15.17
		Firuzjah	30.33	**30.7**	23.5	15.47
	Gilan	Kharfehgil	25.33	27.55	**29.1**	18.02
		Qaleh Rudkhan	24.67	**33.11**	26.62	15.61
		Hashtpar	22.88	**30.24**	29.83	17.07
Semi-humid	Golestan	Aqqala	27.78	**29.27**	26.23	16.73
		Maraveh Tappeh	22.73	**31.35**	28.55	17.38
		Minudasht	24.54	**27.74**	27.64	20.1
	KvB	Pataveh	**26.8**	22.07	26.15	24.98
		Tang Berim	23.41	24.35	**27.79**	24.46
		Yasuj	20.35	25.94	26.85	**26.86**
Semi-arid	E-Az	Tabriz	23.24	20.62	**36.79**	19.36
		Heris	22.9	**27.19**	24.91	25.01
		Sarab	27.1	**28.52**	20.89	23.5
		Liqvan	22.29	**29.69**	23.35	17.74
More than 12 h						
Humid	Mazandaran	Sari	25.67	**30.75**	27.89	15.69
		Abbas Abad	25.6	**29.2**	24.42	20.78
		Firuzjah	**29.17**	28.19	24.35	18.29
	Gilan	Kharfehgil	29.98	**31.04**	22.63	16.36
		Qaleh Rudkhan	24.66	**30.2**	29.05	16.09
		Hashtpar	26.84	**30.4**	26.75	16.01
Semi-humid	Golestan	Aqqala	24.75	**30.26**	24.28	20.71
		Minudasht	25.5	**29.05**	26.45	19.02
	KvB	Pataveh	22.15	20.36	**30.14**	27.35
		Tang Berim	21.01	25.24	**27.13**	26.62
		Yasuj	22.96	**29.56**	26.04	21.44
Semi-arid	E-Az	Tabriz	**34.55**	20.51	28.2	16.75
		Heris	22.55	**33.93**	24.01	19.51
		Sarab	**32.97**	16.6	25.08	25.36

Table 2 (continued)

Climate	Province	Station	Quartile			
			First	Second	Third	Fourth
	Liqvan	14.23		28.73	**39.8**	17.24

Table 3 Results of the compared percentages of rainfall in different climates of Iran

	Climates		
	Humid vs. semi-humid	Humid vs. semi-arid	Semi-humid vs. semi-arid
Less than 6 h			
First quartile	Same	Same	Same
Second quartile	Same	Same	Same
Third quartile	Same	Same	Same
Fourth quartile	Same	Same	Same
6–12 h			
First quartile	SAME	SAME	same
Second quartile	Same	Same	Same
Third quartile	Same	Same	Not same
Fourth quartile	Not same	Not same	Same
More than 12 h			
First quartile	Same	Not same	Not same
Second quartile	Not same	Not same	Not same
Third quartile	Same	Same	Same
Fourth quartile	Not same	Same	Same

Table 4 Binary codes of the selected stations using the first mode (Median Huff curve or SRP) vs. 1:1 line (or USRP) in the three duration-based classes

Climate type	Province	Station	< 6 h	6–12 h	> 12 h
Humid	Mazandaran	Sari	0111	1111	0111
		Abbas Abad	1111	1111	1111
		Firuzjah	0111	1111	1111
	Gilan	Kharfehgil	0111	1111	1111
		Qaleh Rudkhan	0111	0111	0111
		Hashtpar	0111	0111	0111
Semi-humid	Golestan	Aqqala	0111	1111	0111
		Maraveh Tappeh	0111	0111	*
		Minudasht	0011	0111	0111
	KvB	Pataveh	0111	1101	0001
		Tang Berim	0111	0000	0001
		Yasuj	0011	0001	0111
Semi-arid	E-Az	Tabriz	1111	0011	1111
		Heris	0111	0001	0011
		Sarab	1111	1111	1110
		Liqvan	1111	1111	0011

In the greater than 12-h class of storms, there was a statistically significant difference in the averages of dimensionless rainfalls received in the first and second quartiles between the climates, except for a distinct case. This case was a pair of humid and semi-humid climates, which showed no significant difference in the dimensionless rain received in the first quartile. In the third and fourth quartiles (except in the case of a pair of humid and semi-humid climates, in the fourth quartile), there was no statistically significant difference in the averages of dimensionless rainfall depths between the pairs of climates.

Binary method

First mode approach

Table 4 represents the rainfall types of the stations in three classes using the binary method (first mode approach). As can be seen from the table, in the humid climate, for the first class (less than 6 h), the dominant code for most stations was 0111. However, in the second class (6–12 h), the dominant code in most stations was 1111. In the third class (> 12 h), the dominant code was either 1111 or 0111. In the semi-humid climate, for all three rainfall classes, the dominant code of most stations was 0111. In the semi-arid climate, for the first class (less than 6 h) and the second class (6–12 h), the most dominant result was 1111. However, in the third class (> 12 h), the dominant code was 0011. These, based on the 50% Huff curve and the 1:1 line, are consistent with the results of Terranova and Iaquinta (2011), who worked in the Calabria station (with a humid climate) in southern Italy. They reported 1111 as the dominant type of storm in the mentioned site.

Second mode approach

Table 5 depicts the precipitation codes with the highest frequency observed for each of the classes. This table includes all codes that had more than 10% of events in each class. According to Table 5, the binary code 1111 and the code 0000 had the highest frequency among all 16 possible codes. This result is consistent with the results of Terranova and Iaquinta (2011) and Dolsak et al. (2016). In a humid climate (except the Qaleh Rudkhan station for the storms with less than 6 h, where the binary code 0111 had the highest

Table 5 The most observed BSC types in different rainfall classes: a) less than 6 h, b) 6–12 h, and c) more than 12 h in the selected stations in three distinct climates of Iran

		Climate Type	Province	Station	Observed BSC	Most observed BSC-type (> 10%) in general
			< 6 h	6–12 h	> 12 h	
Humid	Mazandaran	Sari	1111 (44.64)	1111 (45.65)	1111 (34.85)	1111,0000,0001,0011,0111
		Abbas abad	1111 (48.57)	1111 (40.43)	1111 (35.29)	1111,0111,0000,0011
		Firuzjah	1111 (30.43)	1111 (52.38)	1111 (44.79)	1111,0000,0111,0011,0001
	Gilan	Kharfehgil	1111 (36.36)	1111 (45.45)	1111 (36)	1111,0011,0111,1110,0001
		Qaleh Rudkhan	0111 (19.05)	1111 (29.69)	1111 (30.23)	1111,0111,0011,0000,0001
		Hashtpar	1111 (35.14)	1111 (28.89)	1111 (30)	1111,0011,0111,0001,0000
Semi-humid	Golestan	Aqqala	1111 (31.58)	1111 (53.85)	1111 (34.62)	1111,0000,0111,0011,0001
		Maraveh Tappeh	1111 (43.18)	1111,0011 (30,30)	……	1111, 0000, 0011,0111,0001
		Minudasht	1111 (33.33)	1111 (39.47)	0111 (31.82)	1111, 0111,0000, 0011,0001
	KvB	Pataveh	1111 (36.36)	1111 (32)	0000 (28.57)	1111,0000,0001,0111,1000,0011
		Tang Berim	1111,0000 (32,32)	0000,1100 (18.18,18.18)	0000 (21.74)	0000,1111,1100,0001,0011,0111
		Yasuj	0000 (42.86)	0000 (37.5)	1111 (35.71)	0000,1111,0111,0001,0011
Semi-arid	E-Az	Tabriz	1111 (44)	0111,0001 (20,20)	1111 (42.86)	1111,0001,0111,1101,0000,1100
		Heris	1111 (38.19)	1111 (29.03)	0111 (27.27)	1111,0111,0011,0000,1011,0001,1000
		Sarab	1111 (50.62)	1111 (29.41)	1111,0000 (40,40)	1111,0000,1000, 0001,1001
		Liqvan	1111 (32.59)	1111 (44)	0000 (37.5)	1111,0000,0011,0111,1000,0001

percentage of storms), the most frequent code was 1111 for all stations and all three precipitation classes. This result was consistent with the findings of Dolsak et al. (2016) in Slovenia. Because the highest code observed in their study for storms lasting less than 12 h was 1111. Likewise, Terranova and Iaquinta (2011) reported that the Calabria station, located in a humid climate part of Italy, binary code 1111, had the highest frequency. This is also consistent with the results of this study.

For the semi-humid climate, it was observed that for all the stations of Golestan province, except Minudasht station, for storms of more than 12 h, binary code 1111 accounted for the highest percentage of storms in all three precipitation classes. At the Maraveh Tappeh station, for precipitation events lasting 6–12 h, the codes 1111 and 0011 were most frequent, and events lasting more than 12 h were rare. At the Pataveh station, for storms lasting less than 12 h, the dominant code was 1111. However, it was 0000 for storms of more than 12 h. At Tang Berim station, precipitation events lasting less than 12 h yielded codes 1111, 0000, and 1100 as the most frequent. This means that for some storms, a significant part of the precipitation falls at the beginning (codes 1111 and 1100). In others, it happened in the second half of the storm duration (code 0000). Also, at Tang Berim station for storms of more than 12 h, the dominant code was 0000. At Yasuj station, precipitation events lasting less than 12 h constituted a significant portion of the precipitation in the second half of the rainfall duration (code 0000). As the rainfall duration increases, the amount of precipitation received at the event's beginning increases. This is reflected in this study by code 1111 for almost all storms.

In a semi-arid climate, it was observed that for almost all the stations and for precipitation lasting less than 12 h,

most of the storms had the code 1111 (except Tabriz station for storm durations of 6–12 h, where the codes 0111 and 0001 were the dominant types of storms). Likewise, for events lasting longer than 12 h, it was observed that at Tabriz station, code 1111 constituted a significant portion of precipitation. At the Heris station, code 0111 constituted a significant part of the rain, which implies that for most of these storms, a large portion of precipitation falls in the first or second quartile. However, at Liqvan station, a large portion of storms fall at the end of the storm duration (code 0000). At the Sarab station, the most common storm pattern of events belonged to codes 1111 and 0000. Likewise, based on the table mentioned above, it can be concluded that among all three climate regions, the binary codes 1111, 0000, 0011, 0111, and 0001 were more frequent than the others. This finding is consistent with the findings of Terranova and Iaquinta (2011), who revealed that the dominant type of storms had codes of 1111, 0000, 0011, 0111, and 1110. Similarly, the results of the current study are completely consistent with the findings of Dolsak et al. (2016), who studied the precipitation patterns of storms in Slovenia and concluded that the codes 1111, 0000, 0011, 0001, and 0111 are dominant in the region.

Figure 6 displays the histogram of the frequencies of sixteen binary codes for the selected stations. The histogram plots of the average percentage of the frequencies of all sixteen binary codes are shown in a general state without classification. As can be inferred from Fig. 6, in humid climates (panel a) and semi-arid climates (panel c) and related stations of Golestan province in a semi-humid climate (panel b on the left), code 1111 is most common among the 16 binary codes. The lowest percentage was equal to 32% in the E-Az province, and the highest percentage was 42% in Mazandaran province. In KvB province, located in the semi-humid climate (panel b on the right), code 0000 was the most common among the 16 binary codes. In Mazandaran province (a humid climate), the codes 1111, 0111, 0000, 0011, and 0001 accounted for about 87% of precipitation events. In Gilan province (a humid climate), codes 1111, 0011, 0111, 0001, and 0000 accounted for about 85% of the storms. In Golestan province (a semi-humid climate), the codes 1111, 0000, 0111, 0011, and 0001 accounted for 90% of the storms. In KvB province (a semi-humid climate), the codes 0000, 1111, 0111, 0001, and 0011 accounted for about 81% of storms, and in E-Az province (a semi-arid climate), the codes 1111, 0000, 0111, 0011, 0001, and 1000 were 82% of the storms.

Introducing new ratios and station clustering

Figure 7 shows the histogram of the newly defined relative ratios for the selected stations for different rainfall classes. As can be seen from Fig. 7, for all three climates, the I_4/I_1 ratio, i.e., the ratio of the area under the Huff curve of 50% in the fourth quartile to the first quartile, was higher than other ratios; this ratio exceeded 6.5 in all three climates. Also, the lowest ratios belonged to I_4/I_3 and I_3/I_2. The ratios I_4/I_1, I_3/I_1, I_2/I_1, I_4/I_2, I_3/I_2, and I_4/I_3 are ranked from the highest to the lowest values (in all three precipitation classes and all three climates). For precipitation events less than 6 h, in a humid climate, the values of I_4/I_1, I_3/I_1, I_2/I_1, I_4/I_2, I_3/I_2, and I_4/I_3 were equal to 8.48, 6.67, 3.7, 2.29, 1.8, and 1.27, respectively. In the semi-humid climate, these values were 9.01, 6.6, 3.68, 2.43, 1.78, and 1.36. For the semi-arid climate, they were 6.78, 5.42, 3.37, 2.01, 1.6, and 1.23.

In the present study, after obtaining the ordinates of 50% Huff curves, the areas under the curves were obtained in the four quartiles, denoted here as I_1, I_2, I_3, and I_4, respectively. To classify the stations, six new ratios (I_2/I_1, I_3/I_1, I_3/I_2, I_4/I_1, I_4/I_2, I_4/I_3) were defined and used as input for cluster analysis. This method is never used by others in the clustering of stations according to storm patterns.

Clustering analysis results

Figure 8 shows the dendrogram of clustering of selected stations based on the newly introduced ratios at three distinct climates using the Ward and Euclidean methods for three precipitation classes. In these diagrams, the horizontal and vertical axes represent the stations and the Euclidean distance, respectively. The dashed line on each dendrogram represents the distance that separates the stations into distinct clusters. In this diagram, each cluster has a different precipitation pattern from the others, and the stations within a cluster are very similar in precipitation pattern. As seen in Fig. 8a, for events lasting less than six hours, three distinct clusters can be distinguished. The first cluster includes eight stations (Qaleh Rudkhan, Minudasht, Firuzjah, Sari, Aqqala, Pataveh, Liqvan, and Tang Berim), the second cluster includes three stations (Kharfehgil, Hashtpar, and Yasuj), and the third cluster includes five stations (Maraveh Tappeh, Heris, Abbas Abad, Tabriz, and Sarab). According to Fig. 8b, it can be seen that for the 6–12 h precipitation class, there are three distinct clusters; the first cluster includes six stations (Sari, Aqqala, Firuzjah, Abbas Abad, Sarab, and Liqvan), and the second and third clusters each include five stations. The second cluster stations include Kharfehgil, Minudasht, Heris, Tang Berim, and Pataveh, and the third cluster stations include Hashtpar, Maraveh Tappeh, Qaleh Rudkhan, Tabriz, and Yasuj. According to Fig. 8c, for precipitation events more than 12 h, the stations are located in four distinct clusters; the first cluster includes seven stations (Sari, Hashtpar, Heris, Yasuj, Aqqala, Minudasht, and Qaleh Rudkhan), the second cluster includes three stations (Pataveh, Tang Berim, and Abbas Abad), the third

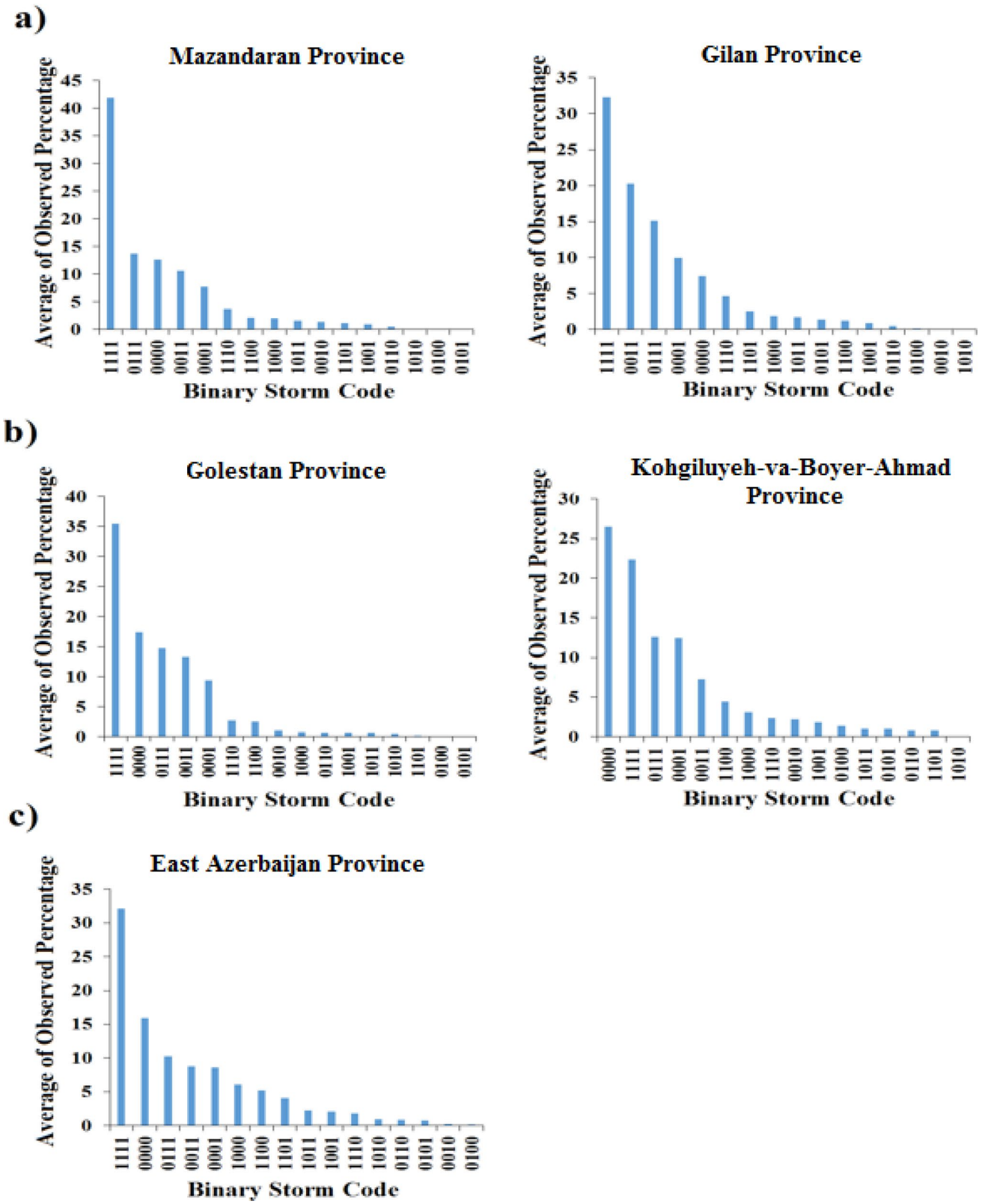

Fig. 6 Histograms of the average percentages of the sixteen binary codes (in general) in the selected stations and the three distinct climates of Iran: **a** humid, **b** semi-humid, and **c** semi-arid

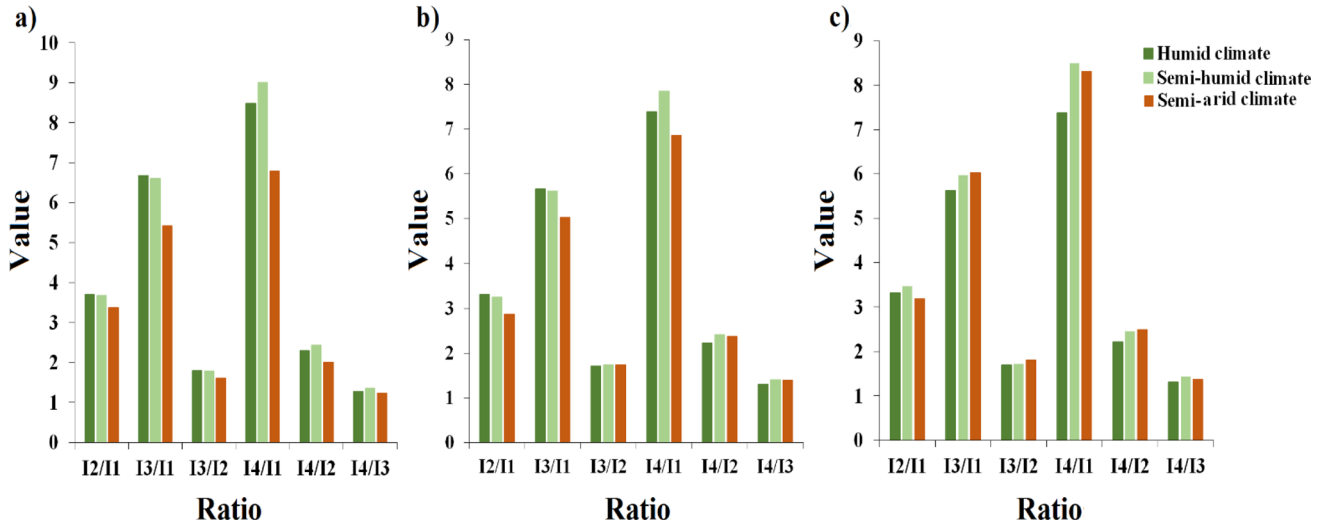

Fig. 7 Histograms of the mean observed ratios for the selected stations in different classes, **a** < 6 h, **b** 6–12 h, and **c** > 12 h in three distinct climates of Iran

cluster includes four stations (Firuzjah, Kharfehgil, Sarab, and Tabriz). The fourth cluster includes one station (Liqvan). Figure 9 shows a set of three distinct maps resulting from clustering analysis. Each figure belongs to a distinct rainfall duration class; Fig. 9a belongs to the less than 6-h class. Similarly, Fig. 9b and Fig. 9c belong to the 6–12 h and greater than 12 h classes, respectively. These figures depict the spatial distribution of clusters in Iran.

Different inputs can be employed for the cluster analysis of stations regarding storm patterns. Wartalska et al. (2020) used the Ward method in cluster analysis of stations in Poland. They used cumulative dimensionless depths in different storms for cluster analysis. Our procedure is somewhat different from that of Wartalska et al. (2020). Moreover, although there are some different similarity measures used for cluster analysis, such as Minkowski distance, Euclidean distance, Manhattan distance, and dynamic time warping (DTW), however, the Euclidean distance is the most widely applied in cluster analysis compared to the others (Wang 2020). Also, this measure is simple for interpretation (Mikolajewski et al. 2022). This is why we used it in the present study. One of the advantages of Ward clustering is the fact that this method does not need to consider the number of subsets before analysis (Wang 2020).

Conclusions

In total, 1983 storms were analyzed in this study in three distinct climate zones of Iran. The data used here consists of rainfall depths over the time period 2001–2019. Sixteen rain gauge stations were selected for analysis. Storms were divided into three precipitation classes based on their duration, which are: (1) < 6 h, (2) 6–12 h, and (3) > 12 h (Fig. 2). Huff curves were plotted for each of the stations and each of the three precipitation classes. The Huff curves were similar in shape and position, with some visual differences depending on the quartile. Using the 50% Huff curve, the percentage of precipitation reached in each quartile was calculated, and the average precipitation in different quartiles and climates was compared.

The binary method was used in two modes. The first mode is based on the 50% Huff curve (SRP) and bisector line (USRP), considering the comparison of I_1, I_2, I_3, and I_4 levels. These correspond to the areas below the 50% Huff curve (SRP) in different quartiles, with the corresponding areas below the 1:1 line (USRP), (Terranova and Iaquinta 2011). The second mode is based on the nondimensional mass curve (NMC) and bisector line (USRP), (Dolsak et al. 2016). Four-digit codes consisting of numbers 0 and 1 were obtained. In the first mode, the results showed that in humid and semi-humid climates, code 0111, and a semi-arid climate, code 1111, had the highest percentage of precipitation patterns. In the second mode, the nondimensional mass curve from each storm showed that, in general, in most precipitation classes, code 1111 and then codes 0000, 0111, 0011, and 0001 constituted a significant part of the precipitation. This finding is consistent with the results of Terranova and Iaquinta's (2011) study for southern Italy and with Dolsak et al. (2016) for Slovenia. New ratios, I_2/I_1, I_3/I_1, I_3/I_2, I_4/I_1, I_4/I_2, and I_4/I_3 were calculated for each of the stations, and the averages of the ratios in each climate and each precipitation class were calculated, and their histogram was drawn. Then, based on the newly introduced ratios, the stations were clustered using Ward's method and Euclidean distance. The results revealed that all the stations could be

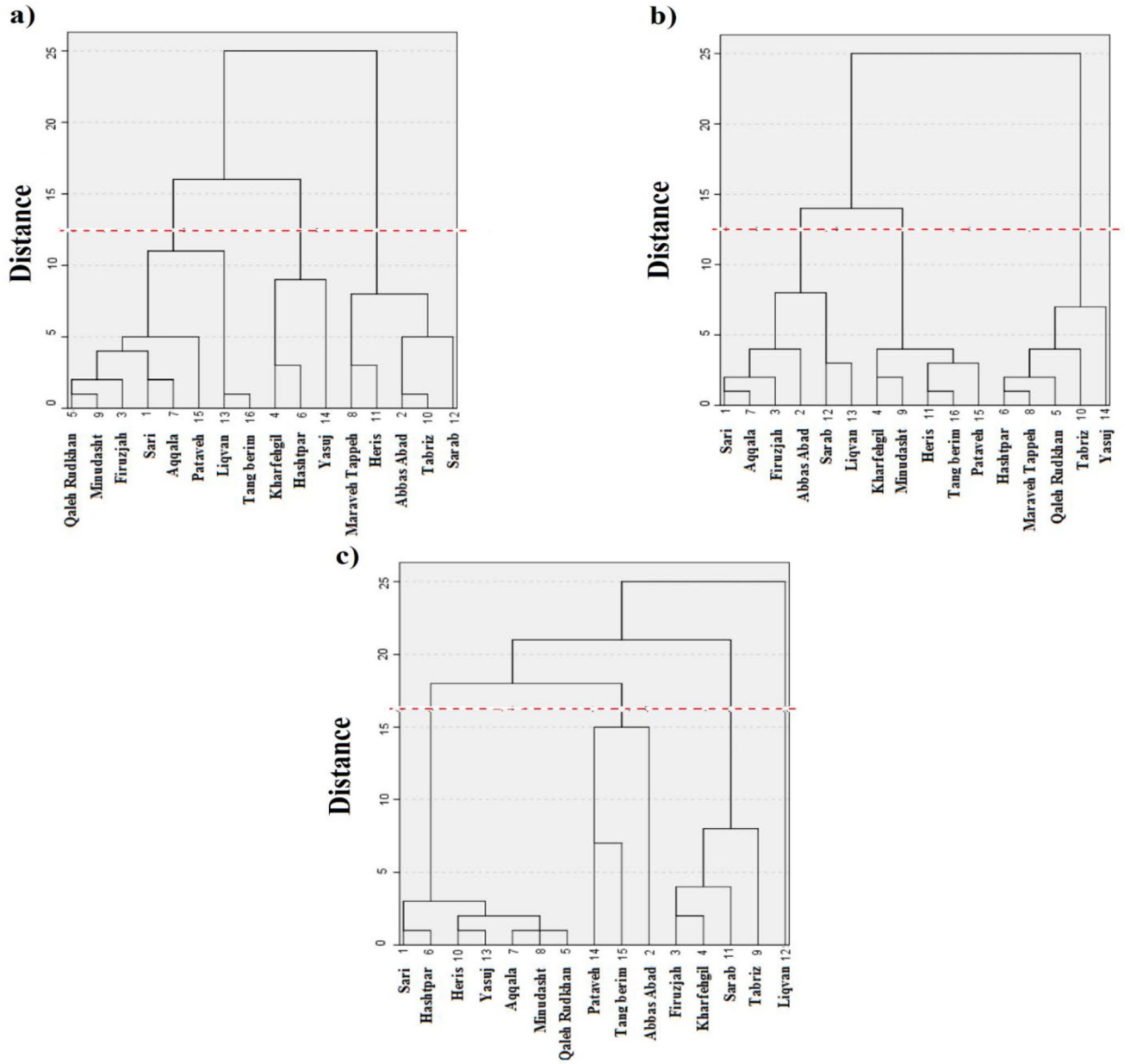

Fig. 8 Dendrograms of the selected stations clustering based on the introduced ratios at three distinct climates using the Ward method and Euclidean distance for different rainfall classes: **a** < 6 h, **b** 6–12 h, and **c** > 12 h

divided into three clusters for less than 6 h and 6–12 h precipitation events, and into four distinct clusters for precipitation events of more than 12 h.

The results of this study were extracted from the available data obtained from the IRAN WRMC. Caution should be taken when using them for practical purposes. As the rain gauge recorder instrument cannot provide a 1-min received depth for snow, snow events are not included. The second limitation is due to the available period of records. This limitation affects the reliability of the results. It is strongly recommended to conduct a similar study every 5 years in the area. The third one is not available with sufficient data for most of the stations. Also, as the arid climate of Iran had a very small number of recorded events (storms), it was not possible to include this climate region in the present study.

The results of this study can be effective in predicting and warning against floods, designing surface drains, and its application in determining the dimensions of hydraulic structures for flood control, construction plans, and planning for drought periods. Likewise, the codes can be used as input for hydrological models (precipitation-runoff). It is

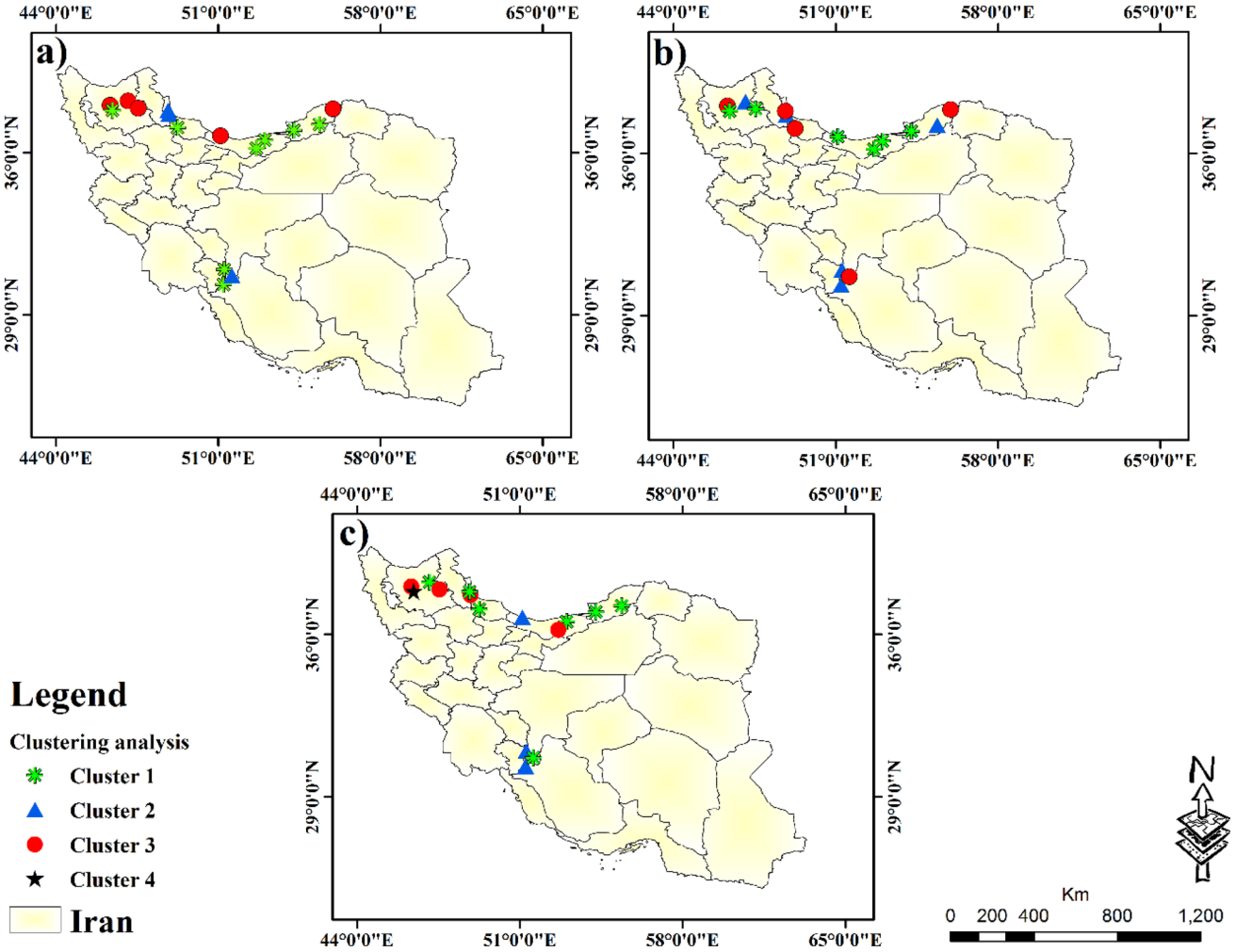

Fig. 9 Three distinct maps resulting from clustering analysis for three duration classes of storms, including **a** < 6 h, **b** 6–12 h, and **c** > 12 h

recommended that for climates around the world with different average annual precipitation, the temporal distribution pattern of precipitation should be investigated and analyzed using the methods presented in this article and other methods, so that it is possible to compare precipitation patterns with different methods.

Acknowledgements We wish to thank the IRAN Water Resources Management Company (IRAN WRMC) for providing the data required to carry out this study. Special thanks are due to the critical and valuable comments of the Editor and two anonymous reviewers. The authors are also thankful to Prof. John Patrick Abraham due improving English.

Author contributions The first draft of the manuscript was prepared by Saina Vakili Azar. Also, she collected the used data and checked the quality of the data. All the figures are plotted by the first and second authors. The second author contributed to the study's conception and design of research. The second and third authors commented on the initial version of the manuscript. All authors read and approved the final version of the manuscript.

Funding The authors declare that no funds, grants, or other support were received during the preparation of this manuscript.

Declarations

Conflict of interest There is no conflict of interest.

References

Abraham J, Stark JR, Minkowycz WJ (2015) Briefing: extreme weather: observed precipitation changes in the USA. Inst Civ Eng 168(2):68–70. https://doi.org/10.1680/feng.14.00015

Alavi ES, Dinpashoh Y, Asadi E (2019) Analysis of hourly storms for the purpose of extracting design hyetographs using the Huff Method. J Geogr Environ Plan 30(3):41–58 (**In Persian with English Abstract**)

Azli M, Rao R (2010) Development of huff curves for Peninsular Malaysia. J Hydrol 388:77–84. https://doi.org/10.1016/j.jhydrol.2010.04.030

Baniasadi M (2011) Experimental investigation of 3D flow over cluster microforms. J Irrigat Water Eng 2(1):62–74 (**In Persian with English Abstract**)

Bazrafshan Daryasari M, Meftah Halghi M, Ghorbani Kh, Ghahraman N (2016) Comparative study of climatic regions of Golestan province under different climate change scenarios. J Water Soil Conserv 22(5):187–202 (**In Persian with English Abstract**)

Bonta JV (2001) Characterizing and estimating spatial and temporal variability of times between storms. Trans ASAE 44(6):1593–1601. https://doi.org/10.13031/2013.7045

Dinpashoh Y, Alavi ES (2024) Derivation of huff curves for the four stations in Great Karun River in Khuzestan province. Journal of Civil and Environmental Engineering 54(1):115–130 (**In Persian with English Abstract**)

Dinpashoh Y, Fakheri-Fard A, Moghaddam M, Jahanbakhsh S, Mirnia M (2004) Selection of variables for the purpose of regionalization of Iran's precipitation climates using multivariate methods. J Hydrol 297:109–123. https://doi.org/10.1016/j.jhydrol.2004.04.009

Dinpashoh Y, Vakili Azar S (2019) Temporal analysis of storms in East of Urmia Lake using the Huff curves. J Water Soil Resour Conserv 8(3):27–44 (**In Persian with English Abstract**)

Dolsak D, Bezak N, Sraj M (2016) Temporal characteristics of rainfall events under three climate types in Slovenia. J Hydrol 541:1395–1405. https://doi.org/10.1016/j.jhydrol.2016.08.047

Dunkerley D (2022) Huff quartile classification of rainfall intensity profiles ('storm patterns'): a modified approach employing an intensity threshold. CATENA 216:106371–106384. https://doi.org/10.1016/j.catena.2022.106371

Ewea A, Elfeki A, Bahrawi J, AL-Amri N (2016) Sensitivity analysis of runoff hydrographs due to temporal rainfall patterns in Makkah Al-Mukkramah region, Saudi Arabia. Arab J Geosci 9:424–435. https://doi.org/10.1007/s12517-016-2443-5

Farsadnia F, Rostami Kamrod M, Moghadam Nia A (2012) Rainfall trend analysis of Mazandaran Province using regional Mann-Kendall test. Iran Water Resour Res 8(2):60–70 (**In Persian with English Abstract**)

Hatami Yazd A, Tagh-Abrishami AA, Ghahraman B (2005) Rainfall temporal pattern for Khorasan province, Iran. Iran Water Resour Res 1(3):54–64 (**In Persian with English Abstract**)

Hirschfield DM (1962) Extreme rainfall relationships. ASCE J Hydraul Div 88(6):73–92

Huff F (1967) Time distribution of rainfall in heavy storms. Water Resour Res 3(4):1007–1019. https://doi.org/10.1029/WR003i004p01007

Huff F (1990) Time distributions of heavy rainstorms in Illinois. In: Illinois state water survey, Champaign, Circular 173

Karimi V, Solaimani K, Habibnejad Roshan M, Shahedi K (2013) Comparison of some rainfall temporal pattern determination for urban flood estimation (Case Study: Babolsar). Iran J Irrigat Water Eng 4(13):102–112 (**In Persian with English Abstract**)

Khaksafidi A, Noura N, Biroudian N, Najafi Nejad A (2011) Rainfall temporal distribution patterns in Sistan and Balouchestan Province (Iran). J Water Soil Conserv 17(1):45–61 (**In Persian with English Abstract**)

Khosravi M, Zahraei A, Heydari H, Bani Naimeh S (2013) Designated drought regions of Gilan using rainfall anomaly index. J Geogr Environ Hazards 1(3):1–20. https://doi.org/10.22067/geo.v1i3.13231. (**In Persian with English Abstract**)

Krvavica N, Rubinic J (2020) Evaluation of design storms and critical rainfall durations for flood prediction in partially urbanized catchments. Water 12:2044–2064. https://doi.org/10.3390/w12072044

Mikolajewski K, Ruman M, Kosek K, Glixelli M, Dzimińska P, Ziętara Z, Licznar P (2022) Development of cluster analysis methodology for identification of model rainfall hyetographs and its application at an urban precipitation field scale. J Sci Total Environ 829:154588. https://doi.org/10.1016/j.scitotenv.2022.154588

Mirabadi A, Noorollahi Y, Almasi M (2017) Geothermal energy resource assessment for greenhouse heating and irrigation (case study: Eastern Azerbaijan province). J Eco Hydrol 4(1):259–274. https://doi.org/10.22059/ije.2017.60908. (**In Persian with English Abstract**)

Mojaradi Gilan H, Ahmadi H, Jaafari M, Bihamta M, Salajegheh A (2010) Study of the temporal distribution pattern of rainfall effect on runoff and sediment generation using rain simulator (Case Study: Alvand Basin). World Appl Sci J 11(1):64–69

Moradnezhadi M, Malekian A, Jourgholami M, Ghasemi A (2016) Daily rainfall temporal distribution patterns and its relations with short-term precipitations in coastal—forest areas (Case Study: Nowshahr Station, Northern Iran). J Range Watershed Manag 69(2):475–485 (**In Persian with English Abstract**)

Nguyen D, Chen ST (2022) Generating continuous rainfall time series with high temporal resolution by using a stochastic rainfall generator with a copula and modified Huff rainfall curves. Water 14:2123–2142. https://doi.org/10.3390/w14132123

Patino C, Molina JL, Espejo F, Zazo S, Mohammad-Hosseinpour A, Silla F (2023) HyetoClust method: hyetograph design through cluster analysis. J Hydrol 625:130014. https://doi.org/10.1016/j.jhydrol.2023.130014

Salas JD (1993) Analysis and modeling of hydrologic time series. In: Maidment DR (ed) Handbook of hydrology. McGraw-Hill, New York

Salehi H, Rezapoor Z, Namjoo K (2017) Climatic zoning of Kohgiluyeh and BoyerAhmad province using factor and cluster analysis. J Clim Res 8(31&32):137–149 (**In Persian with English Abstract**)

Terranova OG, Iaquinta P (2011) Temporal properties of rainfall events in Calabria (Southern Italy). Nat Hazards Earth Syst Sci 11:751–757

Todisco F (2016) The internal structure of erosive and non-erosive storm events for interpretation rainfall simulation. J Hydrol 519:3651–3663. https://doi.org/10.1016/j.jhydrol.2014.11.002

Vakili Azar S, Dinpazhoh Y (2019) Development of Huff curves for the five selected stations in the east of Urmia Lake. J Water Soil 32(6):1109–1123 (**In Persian with English Abstract**)

Wang F (2020) Temporal Pattern Analysis of local rainstorm events in China during the flood season based on time series clustering. Water 12(3):725–733. https://doi.org/10.3390/w12030725

Wang W, Yin S, Xie Y, Liu B, Liu Y (2016) Effects of four storm patterns on soil loss from five soils under natural rainfall. CATENA 141:56–65. https://doi.org/10.1016/j.catena.2016.02.019

Ward JH (1963) Hierarchical grouping to optimize an objective function. J Am Stat Assoc 58(301):236–244

Wartalska K, Kazmierczak B, Nowakowska M, Kotowski A (2020) Analysis of hyetographs for drainage system modeling. J Water 12:149–170. https://doi.org/10.3390/w12010149

Wu SJ, Yang JC, Tung YK (2006) Identification and stochastic generation of representative rainfall temporal patterns in Hong Kong territory. Stoch Environ Res Risk Assess 20:171–183. https://doi.org/10.1007/s00477-005-0245-5

Xlong J, Tang C, Gong L, Chen M (2021) Variability of rainfall time distributions and their impact on peak discharge in the Wenchuan County, China. Bull Eng Geol Env 80:7113–7129. https://doi.org/10.1007/s10064-021-02376-2